catalysts

MDPI

Supporting Information

Phosphate Coordination in a Water-Oxidizing Cobalt Oxide Electrocatalyst Revealed by X-ray Absorption Spectroscopy at the Phosphorus K-Edge

Si Liu, Shima Farhoosh, Paul Beyer, Stefan Mebs, Michael Haumann and Holger Dau *

Department of Physics, Freie Universität Berlin, Arnimallee 14, 14167 Berlin, Germany; liusi@zedat.fu-berlin.de (S.L.); shima.farhoosh@fu-berlin.de (S.F.); paul.beyer@fu-berlin.de (P.B.); stefan.mebs@fu-berlin.de (S.M.); michael.haumann@fu-berlin.de (M.H.)

* Correspondence: holger.dau@fu-berlin.de

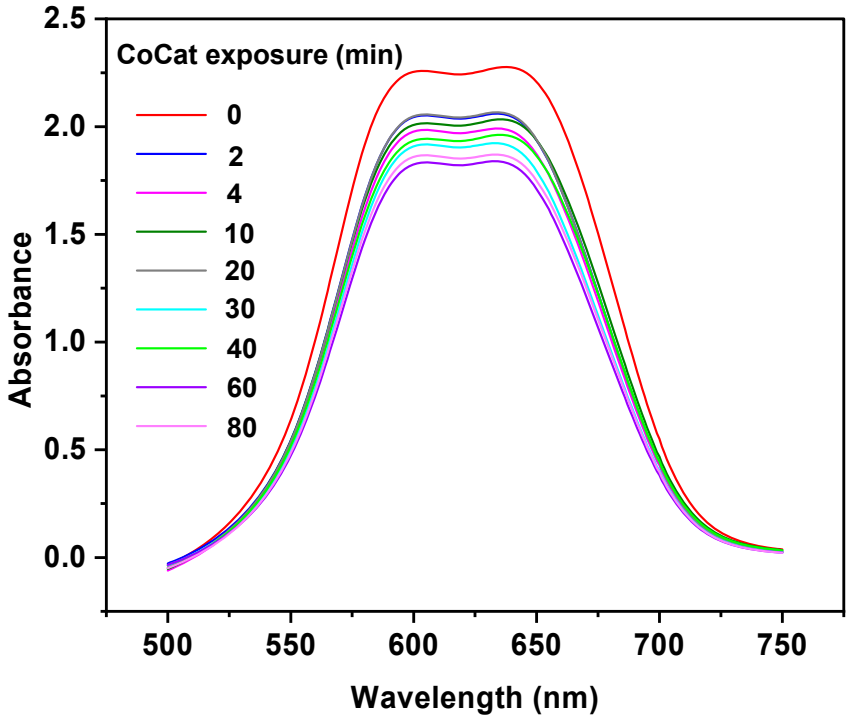

Figure S1. UV−vis absorption spectra of malachite−green/CoCat assay solutions for 100 mC cm^{-2} CoCat samples. Samples were assayed after exposure for the indicated time spans to P-free electrolyte at 1.0 V_{NHE}, CoCat films were dissolved and reacted with the malachite-green assay kit for 30 min (see experimental section) and then the spectra were recorded. The absolute P content in each assay was determined using our earlier reported calibration curve [1]. The total P contents in CoCat films were calculated including the sample dilution steps in the assay procedure.

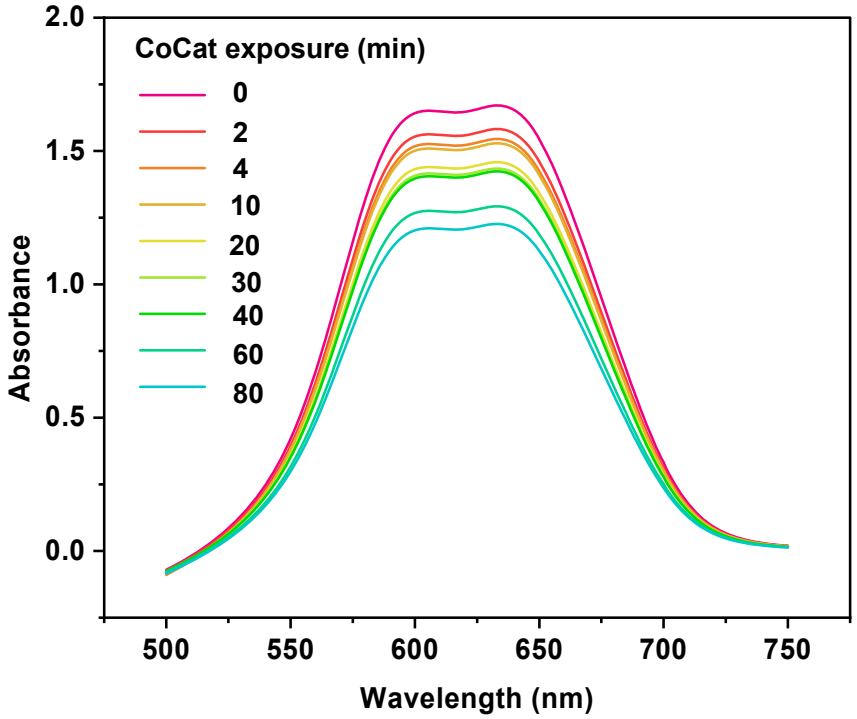

Figure S2. UV−vis absorption spectra of malachite-green/CoCat assay solutions for 20 mC cm^{-2} CoCat samples. Samples were assayed after exposure for the indicated time spans to P−free electrolyte at 1.0 V_{NHE}, CoCat films were dissolved and reacted with the malachite−green assay kit for 30 min (see experimental section) and then the spectra were recorded. Absolute P contents in each assay were determined using our earlier reported calibration curve [1]. The total P contents in CoCat films were calculated including the sample dilution steps in the assay procedure.

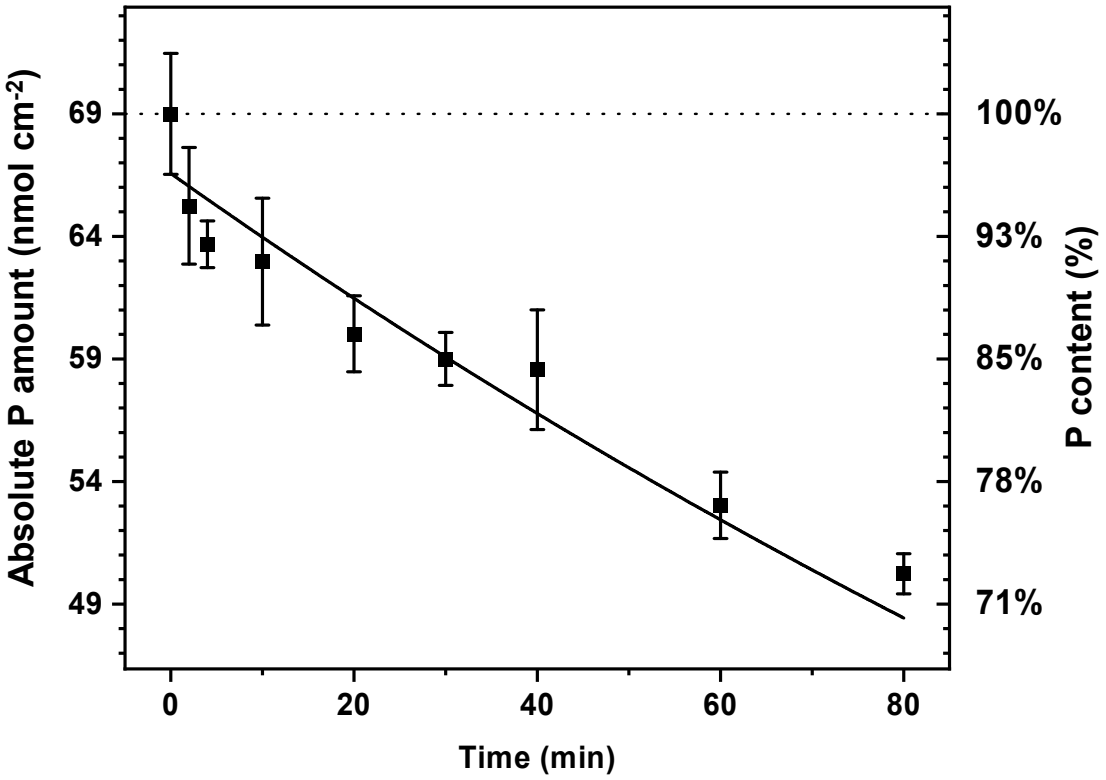

Figure S3. Absolute phosphate contents in CoCat films (20 mC cm^{-2}). The films were operated under the same conditions as described in Figure 1. Each data point (squares) shows the average of at least two individual films with three assays done on each film; error bars show standard deviations. The fit line is a single−exponential decay with a time constant of 250 min and zero offset. For more details see the experimental section.

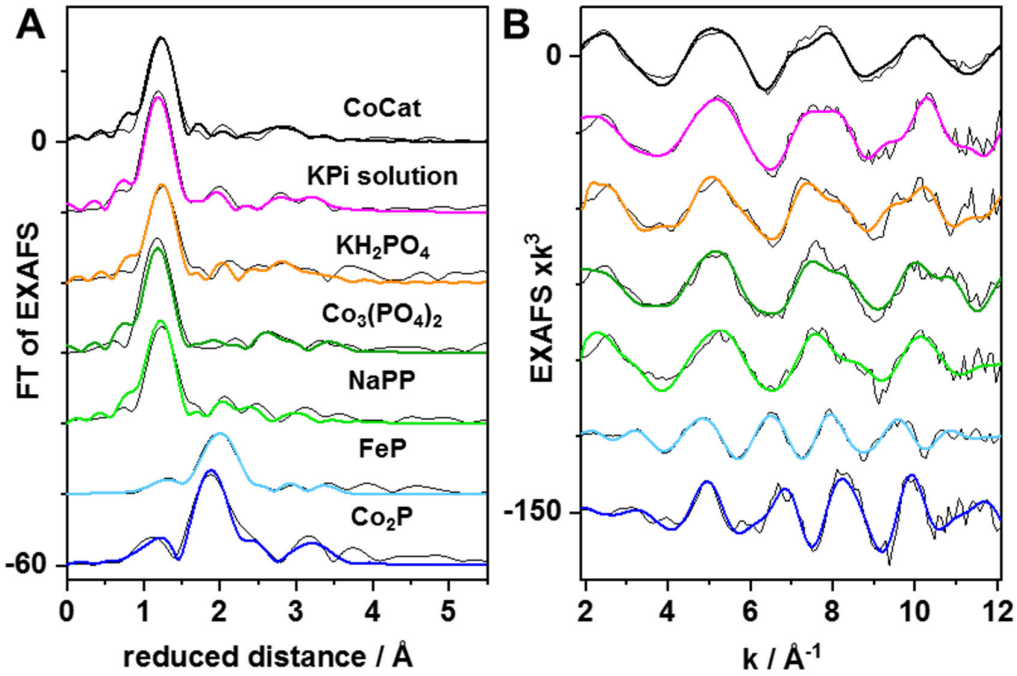

Figure S4. Phosphorus K−edge EXAFS spectra of CoCat and reference compounds. The CoCat spectrum represents the mean of spectra for 50—300 mC cm^{-2} films (Figure 2), reference spectra are for boron−nitride diluted powder samples or an aqueous solution sample (KPi, 2.5 M). (A) Fourier transforms (FT) of P K−edge k^3−weighted EXAFS spectra in (B) (thin black lines, experimental data; thick (colored) lines, simulations with parameters in Tables 1 and S1). Spectra are vertically stacked for clarity. FTs were calculated for k−values of 1.8—12.2 $Å^{-1}$.

Table S1. EXAFS simulation parameters for reference compounds. Coordination number, N [per P]; interatomic distance, R [Å]; Debye−Waller factor, $2\sigma^2$ [Å^2]. *Parameters that were fixed; #, $ denotes coupled parameters to yield a fixed N sum or the same $2\sigma^2$ value for two or more shells. The fit error sum (filtered R−factor, R_F [2]) represents the deviation between data and simulation (in percent) for reduced distances here ranging from 1—3 Å. A 1st−sphere multiple−scattering path contribution (P—O—O) with the expected coordination number of phosphate (PO_4) sites is denoted "ms" (the R−value is the apparent O—O distance). S_0^2 was 0.75. &Partial air oxidation of the grounded FeP and Co_2P powder materials had resulted in phosphorus−oxygen distances in the 1st and 2nd coordination spheres. Distances in parenthesis stem from crystal structures of the respective reference compounds (Figure S6).

	shell	N (per P)	R (Å)	$2\sigma^2$ (Å^2)	R_F (%)
KPi solution 2.5 M	P–O	4*	1.53	0.003#	12.2
	P–O–O_{ms}	6*	2.40	0.003#	
	P– –O	0.2	2.95	0.003#	
	P– –K	1.2	3.17	0.004#	
	P– –K	1.3	3.46	0.004#	
KH_2PO_4	P–O	4*	1.57 (1.55)	0.003#	18.4
	P–O–O_{ms}	6*	2.41 (2.40–2.55)	0.003#	
	P– –O	2.5	2.92 (3.30)	0.003#	
	P– –K	1.9	3.20 (3.34)	0.004#	
	P– –K	1.5	3.47 (3.49)	0.004#	
$Co_3(PO_4)_2$	P–O	4*	1.54 (1.55)	0.004#	17.5
	P–O–O_{ms}	6*	2.43 (2.40–2.55)	0.004#	
	P– –Co	0.8	2.90 (2.70–3.25)	0.005#	
	P– –Co	0.3	3.38 (3.25–3.50)	0.005#	
	P– –O	2.2	3.76 (3.72)	0.005#	
NaPP	P–O	2.1$	1.51 (1.53)	0.001#	19.9
	P–O	1.9$	1.62 (1.67)	0.001#	
	P–O–O_{ms}	6*	2.45 (2.55)	0.002#	
	P– –Na	0.7	2.75 (3.04)	0.002#	
	P– –P	0.3	2.99 (2.98)	0.002#	
	P– –O	1.6	3.29 (3.31)	0.002#	
FeP	P–O&	0.2	1.57	0.002*	7.1
	P–Fe	6.2	2.29 (2.22–2.33)	0.024#	
	P– –P	2.9	2.81 (2.61–3.33)	0.024#	
	P– –Fe	2.9	3.25 (3.23)	0.024#	
	P– –Fe	3.5	3.56 (3.61)	0.024#	
Co_2P	P–O&	0.5	1.52	0.002*	18.6
	P–O&	2.2	2.89	0.002*	
	P–Co	4.9	2.21 (2.14–2.54)	0.012#	
	P– –P	0.9	3.23 (3.27)	0.012#	
	P– –Co	3.5	3.49 (3.47)	0.012#	

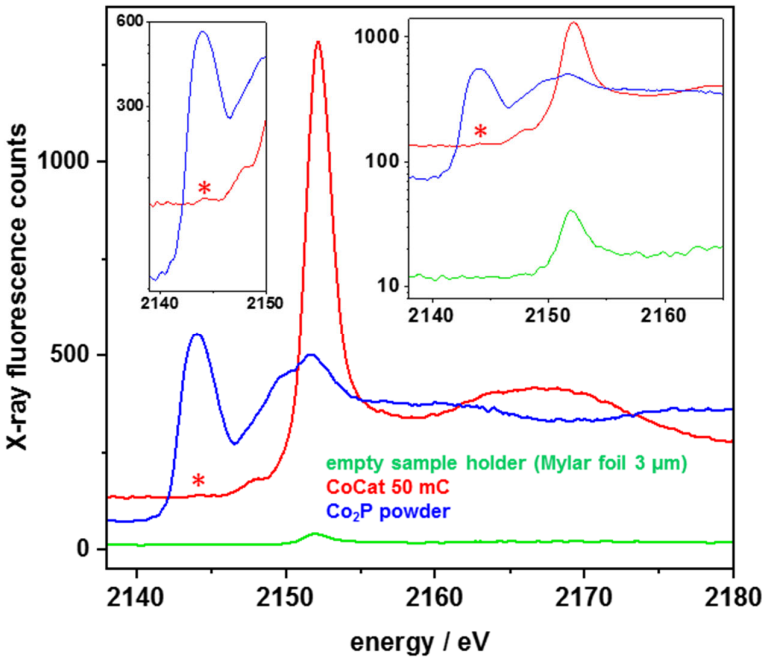

Figure S5. P K−edge XAS spectra. Compared are non-normalized X−ray fluorescence spectra of CoCat (50 mC cm^{-2}), a BN−diluted Co_2P powder sample, and an empty Mylar foil (3 µm)− covered sample holder, all measured at the same (room temperature) conditions. The y−axis shows the average count rate per second for each channel of a 13−element energy−resolving SD−detector. The insets show spectral features in magnification. A small P K−edge is detectable for the Mylar foil, which is insignificant even for the thinnest (50 mC cm^{-2}) CoCat film, and CoCat shows a tiny pre-edge feature at ~2144 eV, similar to the main−edge peak of Co_2P (asterisk).

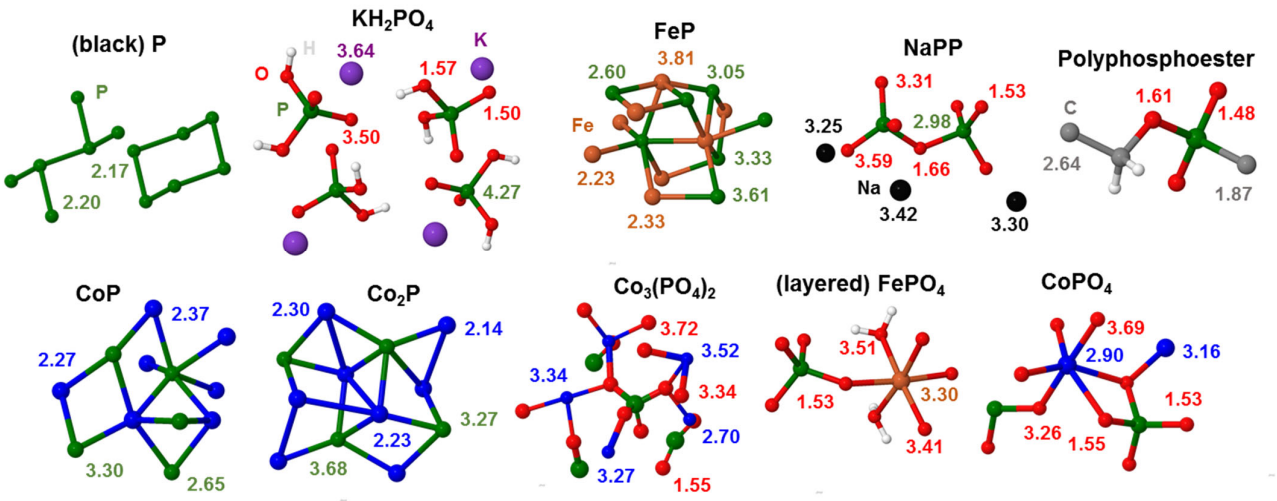

Figure S6. Crystal structures of phosphorus compounds. Displayed are selected cut-outs of structural motifs derived from respective cif files from Internet resources ([3-13]). Bond lengths and longer interatomic distances to P centers with potential relevance for CoCat are compared to respective values from the EXAFS analysis of selected compounds in Table S1. Color code: phosphorus (P), green; oxygen (O), red; potassium (K), purple; iron (Fe), orange; sodium (Na), black; carbon (C), grey; cobalt (Co), blue; hydrogen (H), white. Selected bond lengths and distances (in Å) of atoms to P centers are marked by the respective element colors.

Table S2. Refinement of P−EXAFS simulation parameters for CoCat. Coordination number, N [per P]; interatomic distance, R [Å]; Debye−Waller factor, $2\sigma^2$ [Å^2]; * denotes parameters fixed in the simulation, # marks coupled fitted parameters, Fits I to V represent simulation approaches with increasing complexity. The fit error sum, R_F, was calculated for reduced distances of 1—3 Å. A 1st−sphere multiple−scattering path contribution (P—O—O) with the expected coordination number of phosphate (PO_4) sites is denoted "ms" (the R−value is the apparent O-O distance). S_0^2 was 0.75.

fit	shell	N (per P)	R (Å)	$2\sigma^2$ (Å^2)	R_F (%)
I	P–O	4.0	1.55	0.006	24.4
II	P–O	4*	1.55	0.006#	18.3
	P–O–O_{ms}	6*	2.44	0.006#	
III	P–O	4*	1.55	0.006#	14.5
	P–O–O_{ms}	6*	2.44	0.006#	
	P– –Co	0.6	3.13	0.006#	
IV	P–O	4*	1.55	0.006#	14.0
	P–O–O_{ms}	6*	2.41	0.006#	
	P–Co	0.1	2.25	0.006#	
	P– –Co	0.7	3.13	0.006#	
V	P–O	4*	1.55	0.006#	11.7
	P–O–O_{ms}	6*	2.42	0.006#	
	P–Co	0.1	2.26	0.006#	
	P– –Co	0.7	3.09	0.006#	
	P– –K	0.9	3.30	0.006#	

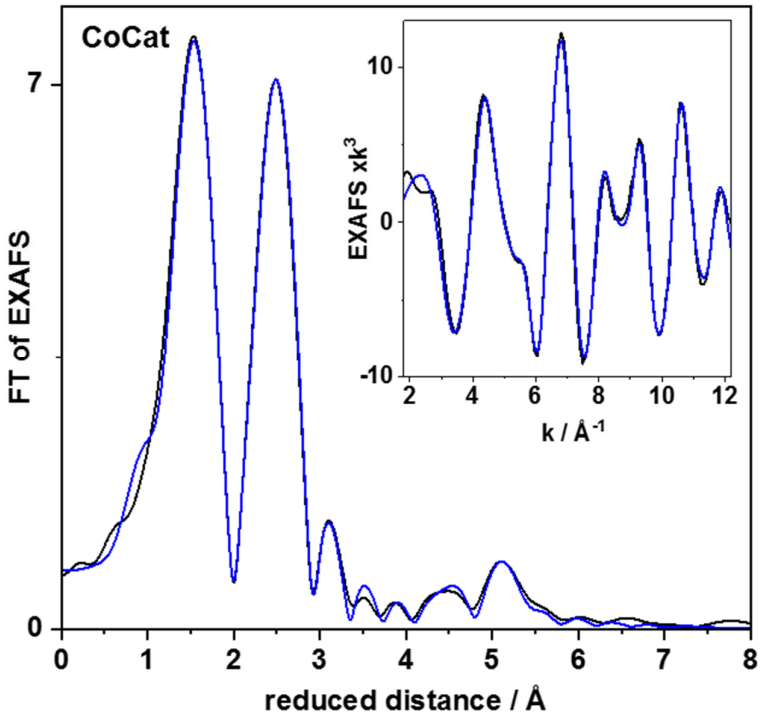

Figure S7. Cobalt EXAFS of CoCat. The CoCat film was 40 mC cm^{-2} thick and the spectrum was collected under operando conditions (KPi, pH 7, room temperature) with an applied potential of 1.1 V_{NHE}. The FT spectrum in the main panel was calculated from the EXAFS spectrum in the inset using a 3.8—12.2 $Å^{-1}$ k−range to emphasize higher−distance FT features. Black lines, experimental data; blue lines, simulation with parameters in Table S3.

Table S3. EXAFS simulation parameters for Co−EXAFS of CoCat. Coordination number, N [per P]; interatomic distance, R [Å]; the Debye−Waller factor, $2\sigma^2$, was set to 0.002 $Å^2$ for all shells; S_0^2 was 0.85; the fit error sum, R_F, in a 1.0—5.5 Å reduced−distance range was 5.9 %.

Shell	Co–O	Co–O	Co–O	Co–O	Co–Co	Co–P	Co–K	Co–O	Co–Co
N	1.7	3.1	0.9	0.6	1.8	0.5	0.3	1.9	0.9
R	1.81	1.92	2.32	2.71	2.81	3.09	3.39	4.84	5.49

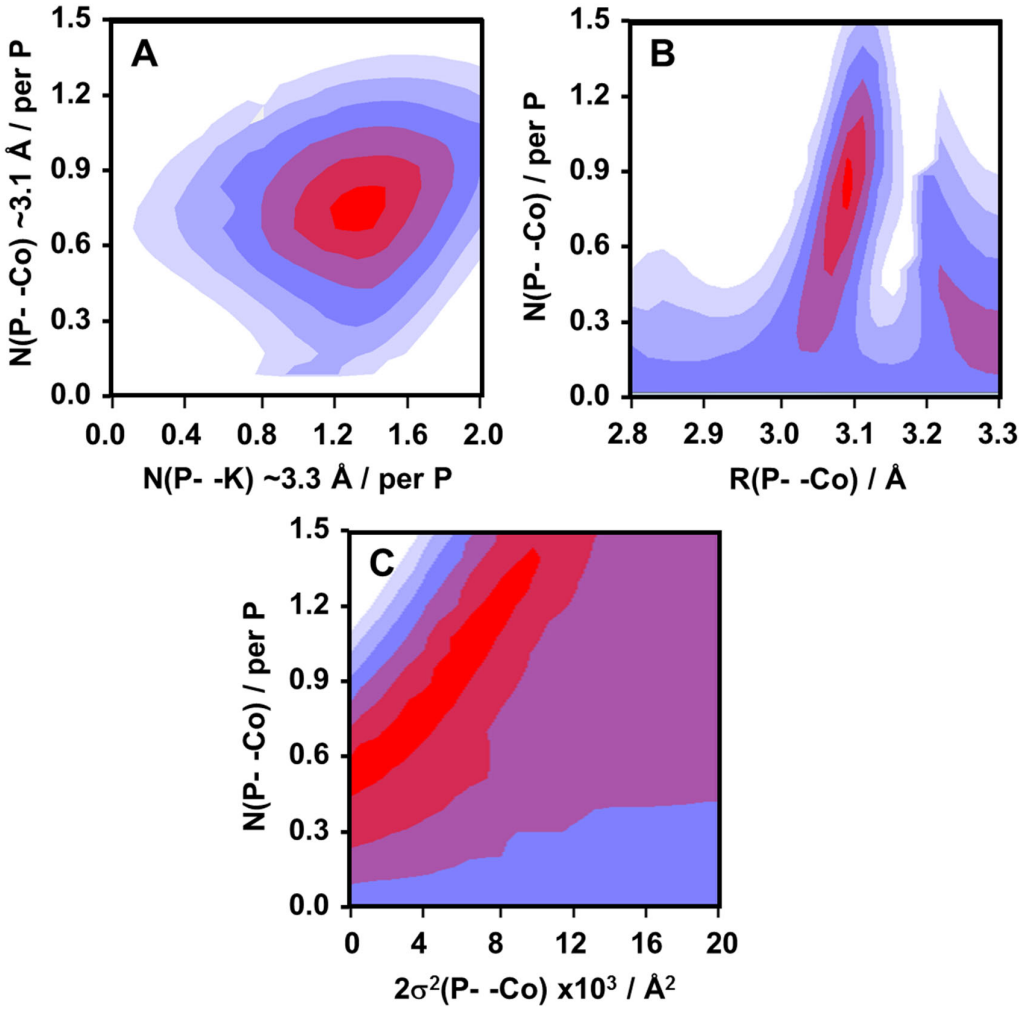

Figure S8. EXAFS fit-error contour plots. Data refer to the mean P K-edge EXAFS spectrum of Co-Cat (Figure 4). Increasingly red colors denote decreasing R_F values meaning increasing fit quality. (A) Correlation of N(P— —Co) and N(P— —K) coordination numbers. (B) Correlation of N(P— —Co) coordination numbers and R(P— —Co) distances (for N(P— —K) = 1.0). (C) Correlation of N(P— —Co) coordination numbers and $2\sigma^2$(P— —Co) Debye-Waller factors (for N(P— —K) = 1.0). R_F values were calculated in a reduced distance range of 2.6—3.3 Å. $2\sigma^2$ for all shells was 0.006 Å² (except for the ~3.1 Å P— —Co distance studied in C).

The EXAFS simulation approach leading to the structural parameters of Table 1 involves determination of the Debye-Waller parameter ($2\sigma^2$ in Table 1) for the P—O distances of the first P coordination sphere, which corresponds to a Gaussian distance distribution function of about 0.05 Å width. We used the same $2\sigma^2$ value also for the Co and K coordination shells (fixed values of $2\sigma^2$ in Table 1). However, the σ-value of these coordination shells likely exceeds 0.05 Å, resulting in underestimated numbers of Co and K atoms at about 3.1 Å (Co) and 3.3 Å (K) in Table 1 (see Panel C on correlation between $2\sigma^2$ and N_{Co}). The problem of underestimating N_{Co} may be further elevated by an asymmetric or even bimodal P—Co distance distribution function with significant contributions from Co ions at distances exceeding 3.2 Å. In conclusion, the value of N_{Co} should be seen as a lower limit.

References

1. Liu, S.; Zaharieva, I.; D'Amario, L.; Mebs, S.; Kubella, P.; Yang, F.; Beyer, P.; Haumann, M.; Dau, H. Electrocatalytic Water Oxidation at Neutral pH–Deciphering the Rate Constraints for an Amorphous Cobalt-Phosphate Catalyst System. *Adv. Energy Mater.*, **2022**, 2202914.
2. Dau, H.; Liebisch, P.; Haumann, M. X-ray absorption spectroscopy to analyze nuclear geometry and electronic structure of biological metal centers - potential and questions examined with special focus on the tetra-nuclear manganese complex of oxygenic photosynthesis. *Anal. Bioanal. Chem.*, **2003**, 376, 562-583.
3. The Materials Project. *Materials Data on FeP by Materials Project*; United States Department of Energy: Washington, DC, USA, 2020.
4. Zheng, T.; Yang, Z.; Gui, D.; Liu, Z.; Wang, X.; Dai, X.; Liu, S.; Zhang, L.; Gao, Y.; Chen, L.; Sheng, D.; Wang, Y.; Diwu, J.; Wang, J.; Zhou, R.; Chai, Z.; Albrecht-Schmitt, T.E.; Wang, S. Overcoming the crystallization and designability issues in the ultrastable zirconium phosphonate framework system. *Nat. Commun.*, **2017**, 8, 15369. https://doi.org/10.1038/ncomms15369.
5. Hultgren, R.; Gingrich, N.S.; Warren, B.E. The Atomic Distribution in Red and Black Phosphorus and the Crystal Structure of Black Phosphorus. *J. Chem. Phys.*, **1935**, 3, 351-355. https://doi.org/10.1063/1.1749671.
6. Endo, S.; Chino, T.; Tsuboi, S.; Koto, K. Pressure-induced transition of the hydrogen bond in the ferroelectric compounds KH_2PO_4 and KD_2PO_4. *Nature*, **1989**, 340, 452-455. https://doi.org/10.1038/340452a0.
7. Leung, K.Y.; Calvo, C. The Structure of $Na_4P_2O_7$ at 22 °C. *Can. J. Chem.*, **1972**, 50, 2519-2526. https://doi.org/10.1139/v72-406.
8. Wyckoff, R.W.G. Second edition. Interscience Publishers, New York, New York Note: cadmium iodide structure. *Cryst. Struct.* **1963**, 1, 239-444.
9. Nord, A.G.; Stefanidis, T. Structure refinements of $Co_3(PO_4)_2$. A note on the reliability of powder diffraction studies. *Acta Chem. Scand. Ser. A*, **1983**, 37, 715-721.
10. Krupkova, R.; Fabry, J.; Vanek, P.; Cisarova, I. Two modifications of a KH_2PO_4.HF adduct. *Acta Cryst. C*, **2003**, 59, i79-i82.
11. Zhou, H.; Upreti, S.; Chernova, N.A.; Whittingham, M.S. Lithium cobalt(II) pyrophosphate, $Li_{1.86}CoP_2O_7$, from synchrotron X-ray powder data. *Acta Cryst. E*, **2011**, 67, i58-i59.
12. Taxer, K.; Bartl, H. On the dimorphy between the variscite and clinovariscite group: refined finestructural relationship of strengite and clinostrengite, $Fe(PO_4) \cdot 2H_2O$. *Cryst. Res. Technol.*, **2004**, 39, 1080-1088. https://doi.org/10.1002/crat.200410293.
13. Jain, A.; Ong, S.P.; Hautier, G.; Chen, W.; Richards, W.D.; Dacek, S.; Cholia, S.; Gunter, D.; Skinner, D.; Ceder, G.; Persson, K.A. Commentary: The Materials Project: A materials genome approach to accelerating materials innovation. *APL Materials*, **2013**, 1, 011002. https://doi.org/10.1063/1.4812323.